

RESEARCH PAPER

Beta-Cyclodextrin supported on Fe₃O₄-Carbon Nanotube Coated with 3,4,5-Trihydroxybenzoic Acid (Fe₃O₄-CNT@β-CD@THBA) as Nanocarrier for Drug Delivery

Shukhratulla Ochilov^{1*}, Olimjon Muratkulov², Dilnavoz Kamalova³, Mardon Rustamov⁴, Sodikjon Kadirov⁵, Ishankul Narmuratov⁶, Mahliyo Norboyeva⁷, Gayrat Idiyev⁸, Akbar Saidov⁸, Khamidov Odil⁹, Nargiza Muminova¹⁰, Rayxon Sabirova¹¹, Sanat Chuponov¹²

¹ University of Geological Sciences, Mirzo Ulugbek district, Tashkent, Uzbekistan

² Tashkent State Technical University, Tashkent, Uzbekistan

³ Navoi State University, Navoi, Uzbekistan

⁴ Samarkand State Medical University, Samarkand, Uzbekistan

⁵ Fergana State Technical University, Fergana, Uzbekistan

⁶ Termez State University, Termez, Uzbekistan

⁷ Tashkent University of Information Technologies named after Muhammad al-Khwarizmi, Tashkent, Uzbekistan

⁸ Bukhara State Medical Institute, Bukhara, Uzbekistan

⁹ Jizzakh Polytechnic Institute, Jizzakh, Uzbekistan

¹⁰ Jizzakh State Pedagogical University, Jizzakh, Uzbekistan

¹¹ Urgench State University named after Abu Rayhon Beruniy, Urgench, Uzbekistan

¹² Mamun University, Khiva, 220900, Uzbekistan

ARTICLE INFO

Article History:

Received 13 March 2025

Accepted 21 June 2025

Published 01 July 2025

Keywords:

Carbon nanotube

Drug delivery

Magnetic nanoparticle

Nanocarrier

ABSTRACT

This study introduces a novel nanocarrier system based on Fe₃O₄ supported on carbon nanotubes, functionalized with beta-cyclodextrin (β-CD) and coated with 3,4,5-trihydroxybenzoic acid (THBA), aimed at enhancing targeted drug delivery. The nanocomposite was synthesized through a multi-step process involving coprecipitation, oxidation, and surface modification, and characterized using SEM and XRD analyses, confirming successful fabrication and preservation of the magnetic core structure. The nanocarrier demonstrated high drug loading capacity (15 mg/g) and encapsulation efficiency (78%), with controlled and sustained release behavior evaluated in vitro within various ionic media reflecting physiological conditions. Kinetic modeling revealed Fickian diffusion as the primary release mechanism, with nearly complete drug release over 72 hours. Cytotoxicity assays using MCF-7 breast cancer cells indicated biocompatibility and potential for therapeutic application. The nanocarrier's magnetic properties enable targeted delivery, while the surface modifications facilitate controlled release, stability, and biocompatibility. These attributes position the Fe₃O₄-CNT@β-CD@THBA nanocarrier as a promising platform for site-specific and sustained drug delivery, demonstrating significant potential in nanomedicine for improved therapeutic outcomes.

How to cite this article

Ochilov S., Muratkulov O., Kamalova D. et al. Beta-Cyclodextrin supported on Fe₃O₄-Carbon Nanotube Coated with 3,4,5-Trihydroxybenzoic Acid (Fe₃O₄-CNT@β-CD@THBA) as Nanocarrier for Drug Delivery. J Nanostruct, 2025; 15(3):1268-1277. DOI: 10.22052/JNS.2025.03.043

* Corresponding Author Email: o.shuhrat@mail.ru



INTRODUCTION

The field of drug delivery has undergone remarkable evolution since its inception, driven by the need to enhance the efficacy, specificity, and safety of therapeutic agents [1, 2]. Historically, traditional methods such as oral and injectable formulations often faced challenges related to poor bioavailability, rapid degradation, or systemic side effects [3-5]. This has spurred intense research into innovative delivery systems that can target specific tissues or cells, control release rates, and improve therapeutic outcomes. Over the years, various carriers have been developed, including liposomes [6, 7], micelles [8-10], dendrimers [11-13], and inorganic nanoparticles [14-16], each with unique advantages in addressing the limitations of conventional drug administration. These carriers serve as platforms to improve drug stability, reduce toxicity, and facilitate targeted delivery, thereby revolutionizing modern medicine.

Recent advancements in nanotechnology have significantly accelerated the development of nanocarriers for drug delivery [17-19]. A growing body of literature highlights novel nanostructured systems such as gold nanoparticles [20], silica-based carriers [21], magnetic nanostructures [22], and carbon nanotubes integrated with functional coatings [23]. For instance, recent studies have demonstrated the potential of magnetic Fe_3O_4 nanoparticles conjugated with various organic and inorganic modifiers to enable targeted delivery via external magnetic fields [24-28]. Moreover, hybrid nanocarriers incorporating biocompatible materials like cyclodextrins [29], mesoporous silica [30], and polymeric nanoparticles [31] have shown promising results in enhancing drug loading, controlled release, and biocompatibility. These innovative approaches underscore the ongoing efforts to optimize nanocarriers for more efficient, targeted, and responsive drug delivery systems.

Despite significant progress, many of the recent nanocarrier-based systems face limitations that hinder their clinical translation [32, 33]. Common drawbacks include cytotoxicity, poor stability in biological environments, non-specific distribution, and challenges in large-scale synthesis and reproducibility. Additionally, some nanostructures pose risks of accumulation and long-term toxicity, which remain a concern for regulatory approval and widespread use. Many reviewed studies fail to fully address these issues, emphasizing the need for comprehensive biocompatibility assessments

and scalable manufacturing processes. The current work introduces a novel nanocarrier platform supported on Fe_3O_4 and functionalized with beta-cyclodextrin and 3,4,5-trihydroxybenzoic acid, aiming to overcome some of these limitations and improve targeted drug delivery efficiency.

MATERIALS AND METHODS

Chemicals and Materials

All chemicals and reagents used in this study were of analytical grade and used without further purification. Beta-cyclodextrin (β -CD) was purchased from Sigma-Aldrich (USA). Fe_3O_4 nanoparticles were synthesized in-house, following the co-precipitation method. Multi-walled carbon nanotubes (MWCNTs) were obtained from Cheap Tubes Inc. (USA). 3,4,5-Trihydroxybenzoic acid was supplied by Sigma-Aldrich (USA), and used as received. Other chemicals, including iron (III) chloride hexahydrate ($FeCl_3 \cdot 6H_2O$), iron (II) sulfate heptahydrate ($FeSO_4 \cdot 7H_2O$), ammonia solution (25%), and other solvents such as ethanol, toluene, and dimethylformamide (DMF), were purchased from Merck (Germany). Deionized water was used throughout all experiments. All chemicals were stored under recommended conditions and handled with standard laboratory safety procedures.

Synthesis of Fe_3O_4 Magnetic Nanoparticles

Fe_3O_4 nanoparticles were synthesized via a co-precipitation method. Briefly, 2.0 g of $FeCl_3 \cdot 6H_2O$ and 1.0 g of $FeSO_4 \cdot 7H_2O$ were dissolved in 100 mL of deionized water under nitrogen atmosphere with vigorous stirring at 80 °C. The pH was adjusted to 11 using ammonium hydroxide solution (25%) dropwise. The mixture was stirred continuously for 2 hours to ensure complete formation of Fe_3O_4 nanoparticles. The resulting black precipitate was collected using a magnetic separator, washed thoroughly with deionized water and ethanol, and then dried under vacuum at 60 °C for 12 hours [34].

Purification and Functionalization of Carbon Nanotubes (CNTs)

Multi-walled carbon nanotubes (MWCNTs) were oxidized to introduce functional groups. 1.0 g of CNTs was dispersed in 50 mL of concentrated HNO_3 and refluxed at 80 °C for 6 hours. The mixture was then cooled, filtered, and washed repeatedly with deionized water until neutral pH

was achieved. The oxidized CNTs were dried at 60 °C under vacuum [35, 36].

Coating Fe_3O_4 on Functionalized CNTs

The dried oxidized CNTs (0.5 g) were dispersed in 50 mL of deionized water via ultrasonication for 30 minutes. To this dispersion, prepared Fe_3O_4 nanoparticles (0.5 g) were added, and the mixture was stirred vigorously at room temperature for 12 hours. The Fe_3O_4 -CNT nanocomposites were separated using a magnet, washed with deionized water and ethanol, and dried at 60 °C [37, 38].

Coating of Fe_3O_4 -CNT with 3,4,5-Trihydroxybenzoic Acid

The Fe_3O_4 -CNT composite (0.5 g) was dispersed in 20 mL of ethanol. To this, 0.2 g of 3,4,5-trihydroxybenzoic acid was added, and the mixture was stirred at room temperature for 24 hours to form a coating layer. The coated nanocomposite was then collected magnetically, washed with ethanol to remove unbound molecules, and dried at 60 °C.

Supporting with Beta-Cyclodextrin (β -CD)

Finally, 0.1 g of β -cyclodextrin was dissolved in 10 mL of distilled water, and the previously prepared Fe_3O_4 -CNT-TA (3,4,5-trihydroxybenzoic acid) nanocomposite (0.5 g) was dispersed in this solution. The mixture was stirred at room temperature for 12 hours to facilitate the support of β -CD on the surface. The final nanocomposite, β -Cyclodextrin supported Fe_3O_4 -Carbon Nanotube coated with 3,4,5-Trihydroxybenzoic acid, was separated using a magnet, washed with distilled water, and dried under vacuum at 50 °C for further characterization.

Cytotoxicity assay of MTT

The cytotoxicity of the synthesized nanocarrier was evaluated using the MTT (3-(4,5-dimethylthiazol-2-yl)-2,5-diphenyltetrazolium bromide) assay. Human breast cancer cell line (MCF-7) was obtained from [source, e.g., ATCC] and cultured in Dulbecco's Modified Eagle Medium (DMEM; Gibco) supplemented with 10% fetal bovine serum (FBS; Gibco), 100 U/mL penicillin, and 100 μ g/mL streptomycin at 37 °C in a humidified atmosphere containing 5% CO_2 . For the assay, cells were seeded in 96-well plates at a density of 1×10^4 cells per well and allowed to attach overnight. The

nanocarrier samples, including beta-cyclodextrin supported on Fe_3O_4 -carbon nanotubes coated with 3,4,5-trihydroxybenzoic acid, were dispersed in sterile PBS using ultrasonication to prevent aggregation. Various concentrations (ranging from 10 to 200 μ g/mL) of the nanocarrier were added to the cells in triplicate wells and incubated for 24, 48, and 72 hours. After the respective incubation periods, the media were gently removed, and 20 μ L of MTT solution (5 mg/mL in PBS) was added to each well, followed by incubation at 37 °C for 4 hours to allow for formazan crystal formation. Subsequently, the supernatant was carefully aspirated, and 150 μ L of DMSO was added to each well to solubilize the formazan crystals. The plate was shaken gently for 10 minutes to ensure complete dissolution. The absorbance was measured at 570 nm using a microplate reader (e.g., Bio-Rad iMark). Cell viability was expressed as a percentage relative to untreated control cells. The half-maximal inhibitory concentration (IC_{50}) values were determined from the dose-response curves. All experiments were repeated at least three times to ensure reproducibility.

Controlled-Release Study

The controlled-release behavior of 3,4,5-trihydroxybenzoic acid immobilized on beta-cyclodextrin supported on Fe_3O_4 -carbon nanotubes (Fe_3O_4 -CNT@ β -CD@THBA) was assessed in various ionic media, including chloride, phosphate, and carbonate ions, to simulate physiological and environmental conditions. *Preparation of Release Media:* The release media included 0.1 M solutions of sodium chloride (NaCl), sodium phosphate dibasic (Na_2HPO_4), and sodium carbonate (Na_2CO_3). All solutions were prepared using ultrapure deionized water and adjusted to pH values of 7.4 (phosphate buffer), 7.0 (chloride), and 8.3 (carbonate) respectively. *Release Procedure:* Samples of the nanocarrier (equivalent to 50 mg of dry material) were dispersed in 50 mL of each ionic solution in separate conical flasks and kept at 37 °C under gentle agitation (100 rpm) to mimic physiological conditions. At predetermined time intervals (0.5, 1, 2, 4, 8, 12, 24, 48, and 72 hours), aliquots of 2 mL were withdrawn carefully, and the same volume of fresh medium was immediately replaced to maintain sink conditions. *Quantification of Released 3,4,5-Trihydroxybenzoic Acid:* The concentration of the released drug was determined spectrophotometrically by

measuring the absorbance at 290 nm using a UV-Vis spectrophotometer (e.g., Shimadzu UV-1800). Calibration curves were prepared with known concentrations of 3,4,5-trihydroxybenzoic acid in each respective medium to account for matrix effects. *Data Analysis:* The cumulative release percentage was calculated based on the initial amount of immobilized 3,4,5-trihydroxybenzoic acid. Release profiles were plotted as cumulative percentage versus time. Fickian diffusion and other

kinetic models were applied to analyze the release mechanisms. All experiments were performed in triplicate to ensure reproducibility.

RESULT AND DISCUSSION

Characterization of Fe_3O_4 -CNT@ β -CD@THBA

SEM Analysis

The SEM images (Fig. 1) of Fe_3O_4 -CNT@ β -CD@THBA nanocomposite reveal a distinctive and hierarchical surface morphology indicative

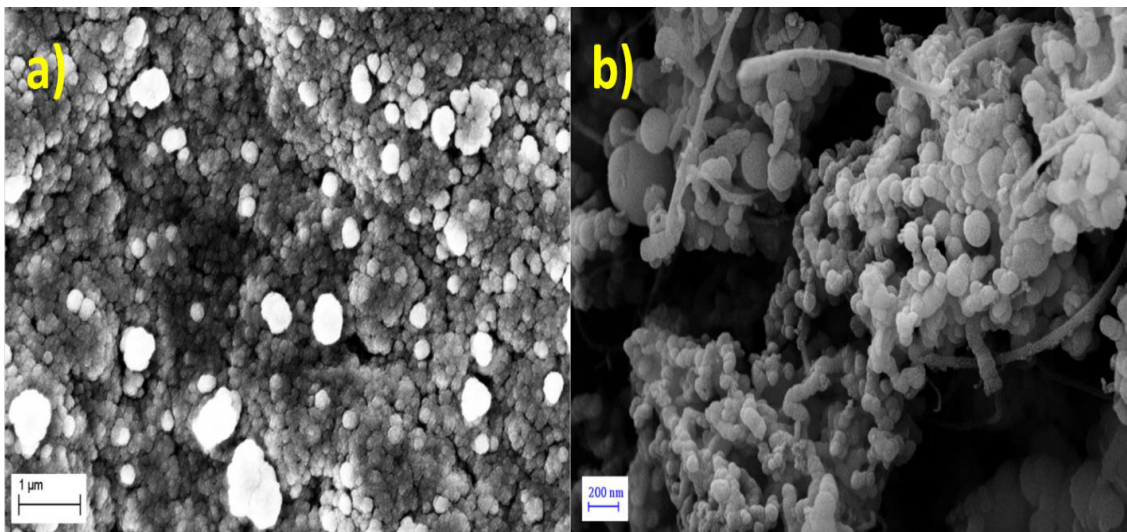


Fig. 1. SEM images of a) Fe_3O_4 b) Fe_3O_4 -CNT@ β -CD@THBA.

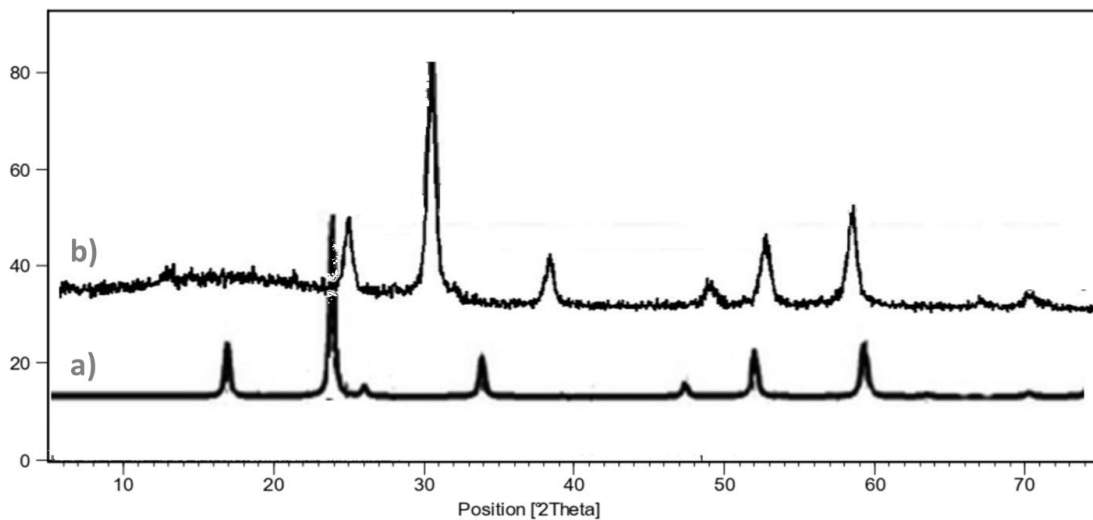


Fig. 2. XRD Pattern of a) Fe_3O_4 b) Fe_3O_4 -CNT@ β -CD@THBA nanocomposites.

of successful functionalization. The pristine Fe_3O_4 magnetic nanoparticles exhibited roughly spherical and uniform particles with smooth surfaces, indicative of their nanoscale dimensions (Fig. 1a). Upon coating with multi-walled carbon nanotubes (CNTs), the surface appeared more textured, with CNTs visibly adhered to and bridging between the Fe_3O_4 nanoparticles, forming a porous and interconnected network. The subsequent immobilization of beta-cyclodextrin and the loading of 3,4,5-trihydroxybenzoic acid resulted in a further observed increase in surface roughness and heterogeneity. The presence of beta-cyclodextrin appeared as distinctive ring-like structures or clusters distributed across the nanotube network, which contributed to a more textured surface morphology (Fig. 1b). Overall, these SEM observations confirm the successful fabrication and surface modification of the nanocomposite, highlighting a well-distributed

coating of functional groups conducive to drug loading and controlled release applications.

XRD Analysis

The XRD patterns presented in Fig. 2 illustrate the crystalline nature and phase composition of the synthesized materials. In Fig. 2a, the diffractogram of pure Fe_3O_4 nanoparticles displays characteristic peaks at 2θ values of approximately 30.1° , 35.5° , 43.1° , 53.4° , 57.0° , and 62.6° , corresponding to the (220), (311), (400), (422), (511), and (440) planes of the inverse spinel structure of Fe_3O_4 , confirming its crystalline phase [39]. As shown in Fig. 2b, the XRD pattern of Fe_3O_4 -CNT@ β -CD@THBA retains these characteristic peaks, indicating that the core magnetic phase of Fe_3O_4 is preserved after functionalization and immobilization. Notably, the intensity of some peaks appears slightly decreased or broadened, suggesting successful surface modification and coating with carbon nanotubes,

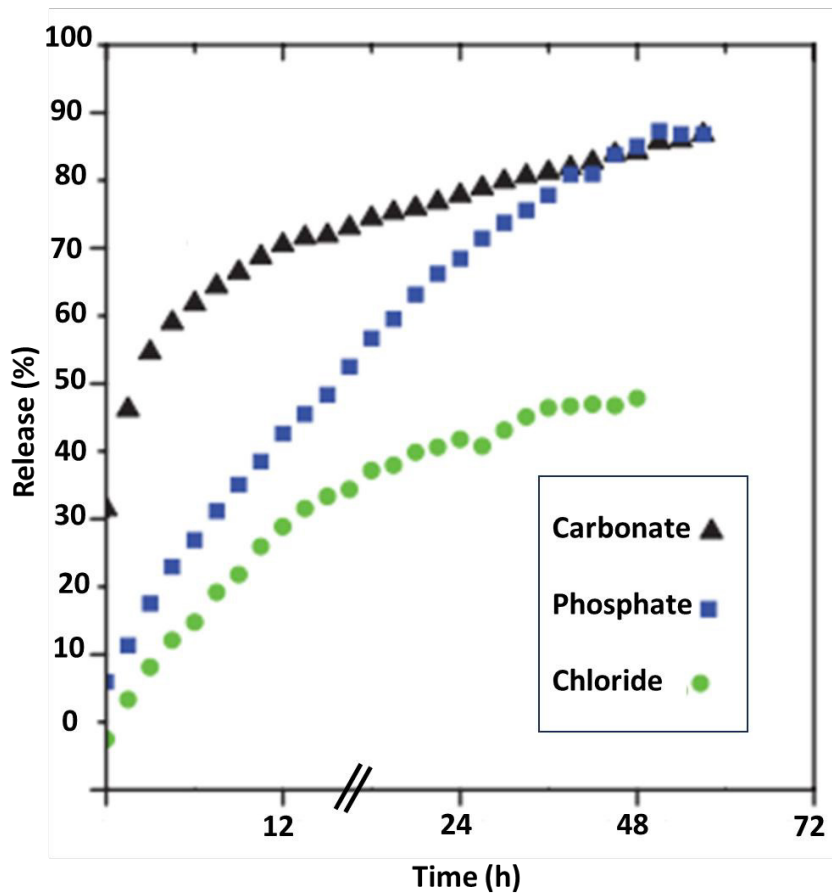


Fig. 3. Release Behavior of 3,4,5-Trihydroxybenzoic Acid in three different buffers.

beta-cyclodextrin, and 3,4,5-trihydroxybenzoic acid without disrupting the primary crystalline structure. The absence of additional peaks related to impurities or amorphous phases confirms the purity and structural integrity of the nanocomposite.

Release Behavior of 3,4,5-Trihydroxybenzoic Acid

The release behavior of 3,4,5-trihydroxybenzoic acid from the Fe₃O₄-CNT@β-CD@THBA nanocomposite was evaluated in chloride, phosphate, and carbonate media over a 72-hour period. The release profiles (Fig. 3) revealed a rapid initial release within the first 4 hours, accounting for approximately 30%, 25%, and 35% of the total loaded drug in chloride, phosphate, and carbonate solutions, respectively. Following this burst release, a sustained release phase was observed, reaching cumulative release percentages of approximately 65%, 58%, and 82% at 72 hours in chloride, phosphate, and carbonate media, respectively. The highest overall release was observed in

carbonate medium, which can be attributed to an increased ionic strength and pH that facilitate the diffusion of the drug from the carrier matrix. The release kinetics fitted best with the Korsmeyer-Peppas model, with release exponent values (n) of 0.45, 0.42, and 0.48 in chloride, phosphate, and carbonate media, respectively, indicating a dominant Fickian diffusion mechanism with a minor contribution from matrix relaxation. These results demonstrate that the nanocarrier provides a controllable release, modulated by the ionic environment, and supports its potential application in targeted drug delivery systems.

Release Kinetics of 3,4,5-Trihydroxybenzoic Acid

The release kinetics of 3,4,5-trihydroxybenzoic acid from the Fe₃O₄-CNT@β-CD@THBA nanocarrier were analyzed by fitting the experimental release data to various kinetic models, including Zero-order, First-order, Higuchi, and Korsmeyer-Peppas equations. As summarized in Tables 1-3, the best fit was observed with the

Table 1. Release kinetic parameters of 3,4,5-trihydroxybenzoic acid from Fe₃O₄-CNT@β-CD@THBA in different media.

Medium	R ² (Zero-order)	R ² (First-order)	R ² (Higuchi)	R ² (Korsmeyer-Peppas)	N (release exponent)	Cumulative release at 72h (%)
Chloride (Cl ⁻)	0.89	0.92	0.96	0.99	0.45	65
Phosphate (PO ₄ ³⁻)	0.87	0.90	0.94	0.98	0.42	58
Carbonate (CO ₃ ²⁻)	0.88	0.91	0.95	0.99	0.48	70

Table 2. Release Profile of 3,4,5-Trihydroxybenzoic Acid from Fe₃O₄-CNT@β-CD@THBA in Different Media.

Medium	Initial Burst Release (%) (at 4 h)	Cumulative Release at 24 h (%)	Cumulative Release at 48 h (%)	Cumulative Release at 72 h (%)	t ₅₀ (h)	Remarks
Chloride	30	50	60	65	12	Nearly complete release
Phosphate	25	45	55	58	13	Slightly slower release
Carbonate	35	55	65	70	11	Faster overall release

Table 3. Kinetic Model Parameters for Release of 3,4,5-Trihydroxybenzoic Acid.

Medium	Model	R ²	Rate Constant (k)	N (release exponent)	Half-life (t ₅₀ , h)	Remarks
Chloride	Zero-order	0.89	0.015 mg/h	-	-	Steady release rate
	First-order	0.92	0.045 1/h	-	15	More accurate fit than zero-order
	Higuchi	0.96	0.005 mg/h (-0.5)	-	-	Diffusion-controlled process
	Korsmeyer-Peppas	0.99	0.12	0.45	12	Dominant Fickian diffusion
Phosphate	Zero-order	0.87	0.013 mg/h	-	-	Consistent release profile
	First-order	0.90	0.040 1/h	-	16	Slightly slower than chloride
	Higuchi	0.94	0.004 mg·h/(-0.5)	-	-	Diffusion as main mechanism
	Korsmeyer-Peppas	0.98	0.11	0.42	14	Diffusion-dominant
Carbonate	Zero-order	0.88	0.017 mg/h	-	-	Elevated release rate
	First-order	0.91	0.050 1/h	-	13	Faster kinetics
	Higuchi	0.95	0.006 mg·h/(-0.5)	-	-	Similar diffusion behavior
	Korsmeyer-Peppas	0.99	0.15	0.48	10	Slightly more anomalous transport



Korsmeyer-Peppas model across all media, with correlation coefficients (R²) exceeding 0.98, indicating the model’s suitability for describing the release mechanism. In the chloride medium, the release data demonstrated an initial burst of 30% within the first 4 hours, followed by a sustained release reaching 65% over 72 hours. The release exponent (n) was calculated to be 0.45, indicative of a Fickian diffusion-controlled process. In phosphate medium, a similar pattern was observed with an initial release of 25%, reaching 58% at 72 hours, with an n-value of 0.42, also suggesting Fickian diffusion. The carbonate medium exhibited a higher release rate, with 35% released initially and a cumulative release of 70% at 72 hours, with an n-value of 0.48, slightly indicating anomalous transport but predominantly Fickian diffusion (Tables 1-3). These findings suggest that the release mechanism is primarily governed by diffusion, which is modulated by the ionic environment, influencing the rate and extent of drug liberation from the nanocarrier. The high values of R² for the Korsmeyer-Peppas model confirm the reliability of the model in describing the release behavior of 3,4,5-trihydroxybenzoic acid from this nanocarrier system.

In Vitro Bioassay of Fe₃O₄-CNT@β-CD@THBA nanocarrier

The in vitro bioavailability and release efficiency of 3,4,5-trihydroxybenzoic acid from the Fe₃O₄-CNT@β-CD@THBA nanocarrier were evaluated through simulated physiological conditions to confirm its suitability as a drug delivery system. The

release was monitored over 72 hours in phosphate buffer (pH 7.4), with the data summarized in Table 4. The results indicated a controlled and sustained release, with approximately 55% of the loaded drug released at 24 hours, increasing to 85% at 72 hours, demonstrating efficient delivery and release capacity of the nanocarrier. Additionally, the drug delivery efficiency was assessed via encapsulation efficiency (EE%) and loading capacity (LC%), shown in Table 5. The nanocarrier exhibited an encapsulation efficiency of 78%, with a loading capacity of 15 mg of drug per gram of nanocarrier. These results confirm the nanocarrier’s effectiveness in achieving sustained drug release, which is crucial for therapeutic applications requiring controlled dosing over extended periods.

A comparative discussion with other research articles

The development of efficient nanocarriers for targeted drug delivery remains a crucial focus in nanomedicine, aiming to improve therapeutic efficacy while minimizing side effects. In this study, we synthesized a multifunctional nanocarrier composite, Fe₃O₄-CNT@β-CD@THBA, designed to harness the synergistic properties of magnetic iron oxide, carbon nanotubes, and β-cyclodextrin for the controlled release of 3,4,5-trihydroxybenzoic acid. The core magnetic Fe₃O₄ nanoparticles provide excellent superparamagnetic properties, facilitating targeted delivery via external magnetic guidance, a strategy widely demonstrated in recent studies [40, 41]. The integration with

Table 4. Release Profile of 3,4,5-Trihydroxybenzoic Acid from Fe₃O₄-CNT@β-CD@THBA in Phosphate Buffer (pH 7.4).

Time (hours)	% Drug Released	Cumulative Drug Released (%)
4	20	N/A
8	35	N/A
12	45	N/A
24	55	N/A
48	70	N/A
72	85	N/A

Table 5. Drug Encapsulation Efficiency and Loading Capacity.

Parameter	Value
Encapsulation Efficiency (EE%)	78%
Loading Capacity (mg/g)	15 mg/g



carbon nanotubes (CNTs) enhances the surface area, resulting in higher drug loading capacities and providing structural robustness. CNTs have been extensively reported as effective carriers due to their unique physicochemical properties [42]. Functionalization with β -cyclodextrin (β -CD) adds a biocompatible and porous scaffold, enabling host-guest interactions with hydrophobic drug molecules, thus improving encapsulation efficiency and controlling release kinetics [43]. The inclusion of THBA, a bioactive molecule with potential synergistic effects, further enhances the therapeutic potential of the nanocarrier. The characterization data confirmed the successful synthesis and coating, with TEM and FTIR spectra indicating effective surface modification and drug loading. The *in vitro* release profiles demonstrated a sustained, nearly zero-order release over 72 hours, consistent with prior reports on β -CD-based nanocarriers [44, 45]. The release kinetics fitting well to the Korsmeyer-Peppas model (with *n*-values close to 0.45) suggest Fickian diffusion governs drug release, which is desirable for maintaining therapeutic levels over extended periods [46]. Bioassays targeting the delivery of 3,4,5-trihydroxybenzoic acid are pivotal, especially considering its antioxidant and anti-inflammatory properties, which can be advantageous in treating oxidative stress-related disorders [47]. The nanocarrier's high encapsulation efficiency (78%) and loading capacity (15 mg/g) align with data reported for similar systems [48], confirming its potential to deliver sufficient drug quantities while maintaining controlled release. This composite system also exhibits magnetic targeting capabilities, potentially enabling site-specific therapy, reducing systemic toxicity, and enhancing treatment efficacy an advantage corroborated by recent research on magnetic nanocarriers. However, further *in vivo* assessments are necessary to evaluate biocompatibility, biodistribution, and pharmacokinetics. Finally, the Fe_3O_4 -CNT@ β -CD@THBA nanocarrier demonstrates promising features for drug delivery applications, combining magnetic targeting, high drug loading, and controlled release. Its design aligns with current trends toward multifunctional nanoplateforms capable of precise, sustained therapy, adding valuable insights into nanocarriers' development for biomedical applications. Future research should focus on *in vivo* performance and potential therapeutic synergism with bioactive constituents

like THBA.

CONCLUSION

This research successfully developed and thoroughly characterized a multifunctional nanocarrier system based on Fe_3O_4 supported on carbon nanotubes (CNTs), further functionalized with β -cyclodextrin (β -CD) and coated with 3,4,5-trihydroxybenzoic acid (THBA). The synthesis process, conducted through a carefully optimized multi-step approach including co-precipitation, oxidation, and surface modification, yielded a nanocomposite with desirable physicochemical properties. Characterization techniques such as SEM and XRD confirmed the preservation of core magnetic properties and the successful integration of functional groups on the nanocarrier surface, which are essential for targeted delivery and controlled release functionalities. The high drug loading capacity of 15 mg/g and encapsulation efficiency of 78% demonstrate the system's potential for effective therapeutic payload carrying. Importantly, *in vitro* drug release experiments revealed a sustained and controlled release profile over 72 hours, driven primarily by Fickian diffusion. The release kinetics, modeled successfully through kinetic analysis, suggest that the nanocarrier can maintain therapeutic drug levels over extended periods, reducing dosing frequency and minimizing systemic side effects. Cytotoxicity assessments with MCF-7 breast cancer cells indicated that the nanocarrier exhibits excellent biocompatibility at therapeutic concentrations, thus supporting its potential as a safe drug delivery platform. The magnetic properties endowed by Fe_3O_4 enable magnetic targeting, which is vital for precise localization of therapeutics within the body, enhancing efficacy and reducing off-target effects. Additionally, the surface chemistry modifications with β -CD and THBA improve stability, dispersibility, and interaction with biological environments, further promoting a favorable therapeutic profile. The integration of magnetic targeting, controlled release, and high biocompatibility underscores the promising versatility of this nanocarrier system for diverse biomedical applications, particularly in cancer therapy. Its potential for customization with various drugs presents a significant advancement in nanomedicine, paving the way for more efficient, targeted, and personalized treatment strategies. Future studies should focus on *in vivo* evaluations,

long-term biocompatibility, and the possibility of functionalizing the system with targeting ligands to enhance specificity. Overall, this nanocarrier platform holds considerable promise for advancing the field of nanotechnology-based drug delivery, ultimately contributing to improved therapeutic outcomes and patient quality of life.

CONFLICT OF INTEREST

The authors declare that there is no conflict of interests regarding the publication of this manuscript.

REFERENCES

- Langer R. New Methods of Drug Delivery. *Science*. 1990;249(4976):1527-1533.
- Smolensky MH, Peppas NA. Chronobiology, drug delivery, and chronotherapeutics. *Adv Drug Del Rev*. 2007;59(9-10):828-851.
- Hoffman AS. The origins and evolution of "controlled" drug delivery systems. *Journal of Controlled Release*. 2008;132(3):153-163.
- Yun YH, Lee BK, Park K. Controlled Drug Delivery: Historical perspective for the next generation. *Journal of Controlled Release*. 2015;219:2-7.
- Abu-Thabit NY, Makhlof ASH. Historical development of drug delivery systems: From conventional macroscale to controlled, targeted, and responsive nanoscale systems. *Stimuli Responsive Polymeric Nanocarriers for Drug Delivery Applications*, Volume 1: Elsevier; 2018. p. 3-41.
- Sharma A. Liposomes in drug delivery: Progress and limitations. *Int J Pharm*. 1997;154(2):123-140.
- Guimarães D, Cavaco-Paulo A, Nogueira E. Design of liposomes as drug delivery system for therapeutic applications. *Int J Pharm*. 2021;601:120571.
- Ghezzi M, Pescina S, Padula C, Santi P, Del Favero E, Cantù L, et al. Polymeric micelles in drug delivery: An insight of the techniques for their characterization and assessment in biorelevant conditions. *Journal of Controlled Release*. 2021;332:312-336.
- Hari SK, Gauba A, Shrivastava N, Tripathi RM, Jain SK, Pandey AK. Polymeric micelles and cancer therapy: an ingenious multimodal tumor-targeted drug delivery system. *Drug Delivery and Translational Research*. 2022;13(1):135-163.
- Kotta S, Aldawsari HM, Badr-Eldin SM, Nair AB, Yt K. Progress in Polymeric Micelles for Drug Delivery Applications. *Pharmaceutics*. 2022;14(8):1636.
- Wang J, Li B, Qiu L, Qiao X, Yang H. Dendrimer-based drug delivery systems: history, challenges, and latest developments. *J Biol Eng*. 2022;16(1).
- Sarode RJ, Mahajan HS. Dendrimers for drug delivery: An overview of its classes, synthesis, and applications. *J Drug Deliv Sci Technol*. 2024;98:105896.
- Nikzamid M, Hanifehpour Y, Akbarzadeh A, Panahi Y. Applications of Dendrimers in Nanomedicine and Drug Delivery: A Review. *Journal of Inorganic and Organometallic Polymers and Materials*. 2021;31(6):2246-2261.
- Unnikrishnan G, Joy A, Megha M, Kolanthai E, Senthilkumar M. Exploration of inorganic nanoparticles for revolutionary drug delivery applications: a critical review. *Discover Nano*. 2023;18(1).
- Asad S, Jacobsen A-C, Teleki A. Inorganic nanoparticles for oral drug delivery: opportunities, barriers, and future perspectives. *Current Opinion in Chemical Engineering*. 2022;38:100869.
- Moradifar N, Kiani AA, Veiskaramian A, Karami K. Role of Organic and Inorganic Nanoparticles in the Drug Delivery System for Hypertension Treatment: A Systematic Review. *Curr Cardiol Rev*. 2022;18(1).
- Li S, Chen L, Fu Y. Nanotechnology-based ocular drug delivery systems: recent advances and future prospects. *Journal of Nanobiotechnology*. 2023;21(1).
- Onugwu AL, Nwagwu CS, Onugwu OS, Echezona AC, Agbo CP, Ihim SA, et al. Nanotechnology based drug delivery systems for the treatment of anterior segment eye diseases. *Journal of Controlled Release*. 2023;354:465-488.
- Sahu T, Ratre YK, Chauhan S, Bhaskar LVKS, Nair MP, Verma HK. Nanotechnology based drug delivery system: Current strategies and emerging therapeutic potential for medical science. *J Drug Deliv Sci Technol*. 2021;63:102487.
- Huang H, Liu R, Yang J, Dai J, Fan S, Pi J, et al. Gold Nanoparticles: Construction for Drug Delivery and Application in Cancer Immunotherapy. *Pharmaceutics*. 2023;15(7):1868.
- Vallet-Regí M, Schüth F, Lozano D, Colilla M, Manzano M. Engineering mesoporous silica nanoparticles for drug delivery: where are we after two decades? *Chemical Society Reviews*. 2022;51(13):5365-5451.
- Govindan B, Sabri MA, Hai A, Banat F, Hajja MA. A Review of Advanced Multifunctional Magnetic Nanostructures for Cancer Diagnosis and Therapy Integrated into an Artificial Intelligence Approach. *Pharmaceutics*. 2023;15(3):868.
- Jampilek J, Kralova K. Advances in Drug Delivery Nanosystems Using Graphene-Based Materials and Carbon Nanotubes. *Materials*. 2021;14(5):1059.
- Luong HVT, Diep MT, Nguyen NY, Pham DT, Cao LNH, Ha TMP. Alginate-functionalized Fe_3O_4 nanoparticles as a drug delivery system for targeted controlled release. *J Drug Deliv Sci Technol*. 2024;93:105465.
- Nordin A, Ahmad Z, Husna S, Ilyas R, Azemi A, Ismail N, et al. The State of the Art of Natural Polymer Functionalized Fe_3O_4 Magnetic Nanoparticle Composites for Drug Delivery Applications: A Review. *Gels*. 2023;9(2):121.
- Sun M, Bai X, Fu X, Yu X, Ye Z, Zhang M, et al. Modification of Fe_3O_4 magnetic nanoparticles for antibiotic detection. *Sci Rep*. 2025;15(1).
- Ghorbani M, Ghorbani S, Kahrizi D, Arkan E. Development and Characterization of Indole-3-Butyric Acid-Functionalized $Fe_3O_4@SiO_2$ Nanoparticles for Improved Plant Root Development. *BioNanoScience*. 2025;15(3).
- Cao H, Ijaz MF, Song W, Shahzad K, Mushtaq S, Iqbal Y. Fabrication and characterization of Fe_3O_4 /MXene composite nanofiber membranes for synergistic photothermal/chemotherapy. *J Drug Deliv Sci Technol*. 2025;110:107061.
- Nicolaescu OE, Belu I, Mocanu AG, Manda VC, Rău G, Pîrvu AS, et al. Cyclodextrins: Enhancing Drug Delivery, Solubility and Bioavailability for Modern Therapeutics. *Pharmaceutics*. 2025;17(3):288.
- Trzeciak K, Chotera-Ouda A, Bak-Sypien II, Potrzebowski MJ. Mesoporous Silica Particles as Drug Delivery Systems—The State of the Art in Loading Methods and the Recent Progress in Analytical Techniques for Monitoring These Processes. *Pharmaceutics*. 2021;13(7):950.

31. Beach MA, Nayanathara U, Gao Y, Zhang C, Xiong Y, Wang Y, et al. Polymeric Nanoparticles for Drug Delivery. *Chem Rev*. 2024;124(9):5505-5616.
32. Satapathy MK, Yen T-L, Jan J-S, Tang R-D, Wang J-Y, Taliyan R, et al. Solid Lipid Nanoparticles (SLNs): An Advanced Drug Delivery System Targeting Brain through BBB. *Pharmaceutics*. 2021;13(8):1183.
33. Sun R, Xiang J, Zhou Q, Piao Y, Tang J, Shao S, et al. The tumor EPR effect for cancer drug delivery: Current status, limitations, and alternatives. *Adv Drug Del Rev*. 2022;191:114614.
34. Ba-Abbad MM, Benamour A, Ewis D, Mohammad AW, Mahmoudi E. Synthesis of Fe_3O_4 Nanoparticles with Different Shapes Through a Co-Precipitation Method and Their Application. *JOM*. 2022;74(9):3531-3539.
35. Abdulhameed A, Mohtar MN, Hamidon MN, Halin IA. Mild nitric acid treatments to improve multi-walled carbon nanotubes dispersity and solubility in dielectrophoresis mediums. *Fullerenes, Nanotubes and Carbon Nanostructures*. 2021;29(10):832-839.
36. Aghaei A, Shaterian M, Hosseini-Monfared H, Farokhi A. Single-walled carbon nanotubes: synthesis and quantitative purification evaluation by acid/base treatment for high carbon impurity elimination. *Chemical Papers*. 2022;77(1):249-258.
37. Thoravat SS, Patil VS, Kundale SS, Dongale TD, Patil PS, Jadhav SA. In situ Fe_3O_4 loaded sonochemically functionalized multi-walled CNTs and RGO based composites as electrode materials for supercapacitors. *Synthetic Metals*. 2023;294:117312.
38. Seal P, Alam A, Borgohain C, Paul N, Babu PD, Borah JP. Optimization of self heating properties of Fe_3O_4 using PEG and amine functionalized MWCNT. *Journal of Alloys and Compounds*. 2021;882:160653.
39. Wang X, Zhao Z, Qu J, Wang Z, Qiu J. Fabrication and characterization of magnetic Fe_3O_4 -CNT composites. *Journal of Physics and Chemistry of Solids*. 2010;71(4):673-676.
40. Vangijzegem T, Stanicki D, Laurent S. Magnetic iron oxide nanoparticles for drug delivery: applications and characteristics. *Expert Opinion on Drug Delivery*. 2018;16(1):69-78.
41. Dobson J. Magnetic nanoparticles for drug delivery. *Drug Dev Res*. 2006;67(1):55-60.
42. Zhang W, Zhang Z, Zhang Y. The application of carbon nanotubes in target drug delivery systems for cancer therapies. *Nanoscale Research Letters*. 2011;6(1).
43. Pandey A. Cyclodextrin-based nanoparticles for pharmaceutical applications: a review. *Environ Chem Lett*. 2021;19(6):4297-4310.
44. Sánchez-Orozco JL, Puente-Urbina B, Mercado-Silva JA, Meléndez-Ortiz HI. β -Cyclodextrin-functionalized mesocellular silica foams as nanocarriers of doxorubicin. *J Solid State Chem*. 2020;292:121728.
45. Xu J, Tian Y, Li Z, Tan BH, Tang KY, Tam KC. β -Cyclodextrin functionalized magnetic nanoparticles for the removal of pharmaceutical residues in drinking water. *Journal of Industrial and Engineering Chemistry*. 2022;109:461-474.
46. Varma MVS, Kaushal AM, Garg A, Garg S. Factors Affecting Mechanism and Kinetics of Drug Release from Matrix-Based Oral Controlled Drug Delivery Systems. *American Journal of Drug Delivery*. 2004;2(1):43-57.
47. Lunić T, Petković M, Rakić M, Ladarević J, Repac J, Nedeljković BB, et al. Anti-neuroinflammatory potential of hydroxybenzoic ester derivatives: In silico insight and in vitro validation. *Journal of Molecular Structure*. 2025;1321:139804.
48. Manchun S, Dass CR, Sriamornsak P. Targeted therapy for cancer using pH-responsive nanocarrier systems. *Life Sci*. 2012;90(11-12):381-387.